Mercury's plasma environment after BepiColombo's third flyby

Lina Z. Hadid, Dominique Delcourt, Yuki Harada, Mathias Rojo, Sae Aizawa, Yoshifumi Saito, Nicolas André, Austin N. Glass, Jim M. Raines, Shoichiro Yokota, et al.

communications physics

Article

https://doi.org/10.1038/s42005-024-01766-8

Mercury's plasma environment after BepiColombo's third flyby

Lina Z. Hadid[1] ✉, Dominique Delcourt[1,2], Yuki Harada[3], Mathias Rojo[4], Sae Aizawa[1,5,6], Yoshifumi Saito[5], Nicolas André[4,7], Austin N. Glass[8], Jim M. Raines[8], Shoichiro Yokota[9], Markus Fränz[10], Bruno Katra[1], Christophe Verdeil[4], Björn Fiethe[11], Francois Leblanc[12], Ronan Modolo[12], Dominique Fontaine[1], Norbert Krupp[10], Harald Krüger[10], Frédéric Leblanc[1], Henning Fischer[10], Jean-Jacques Berthelier[12], Jean-André Sauvaud[4], Go Murakami[5] & Shoya Matsuda[13]

Understanding Mercury's magnetosphere is crucial for advancing our comprehension of how the solar wind interacts with the planetary magnetospheres. Despite previous missions, several gaps remain in our knowledge of Mercury's plasma environment. Here, we present findings from BepiColombo's third flyby, offering a synoptic view of the large scale structure and composition of Mercury's magnetosphere. The Mass Spectrum Analyzer (MSA), Mass Ion Analyzer (MIA), and Mass Electron Analyzer (MEA) on the magnetospheric orbiter reveal insights, including the identification of trapped energetic hydrogen (H^+) with energies around 20 keV e^{-1} evidencing a ring current, and a cold ion plasma with energies below 50 eV e^{-1}. Additionally, we observe a Low-Latitude Boundary Layer (LLBL), which is a region of turbulent plasma at the edge of the magnetosphere, characterized by bursty ion enhancements, indicating an ongoing injection process in the duskside magnetosphere flank. These observations during cruise phase provide a tantalizing glimpse of future discoveries expected from the Mercury Plasma Particle Experiment (MPPE) instruments after orbit insertion, promising broader impacts on our understanding of planetary magnetospheres.

The space plasma environment of Mercury, the planet closest to the Sun, forms a complex and tightly coupled system with the interior and the surface of the planet. Due to its proximity to our star and to its weak magnetic field, Mercury's surface is subjected to more extreme solar wind conditions than Earth or any other planet[1,2]. The planet's surface, exosphere, and magnetosphere are strongly linked together by various interaction processes (such as thermal desorption and sputtering) that facilitate the escape of planetary material and energy exchange. Ion populations in Mercury's magnetosphere may thus originate either from the impinging solar wind (especially H^+ and He^{2+}) or from the planet via ionization of exospheric neutrals. Mariner 10[3], the first spacecraft to visit Mercury, conducted three flybys and discovered traces of heavy atoms in near Mercury's gravitationally bound exosphere[4]. Later, Earth-based telescopes remotely measured a selection of planetary-originating ions, including sodium (Na^+)[5], potassium (K^+)[6], calcium (Ca^+)[7], and others. Thanks to the Mercury Surface, Space ENvironment, GEochemistry, and Ranging (MESSENGER[8]), spacecraft observations, we now have a better understanding of the ion plasma in Mercury's magnetosphere. The Fast Imaging Particle Spectrometer (FIPS) onboard MESSENGER revealed that this plasma includes both H^+, He^{2+} originating from the solar wind, and heavier species like He^+, O^+-group (mass-per-charge, m/q = 16–20 amu/e including O^+ and water group ions) and Na^+-group (21–30 amu/e, including Na^+, Mg^+, Al^+, and Si^+) of planetary origin[9–11]. While He^+ ions were shown to exhibit a relatively even distribution around the planet, heavier ions (both Na^+-group and O^+-

[1]LPP, CNRS, Observatoire de Paris, Sorbonne Université, Université Paris Saclay, École polytechnique, Institut Polytechnique de Paris, Palaiseau, France. [2]LPC2E-CNRS-CNES-Orléans University, Orléans, France. [3]Department of Geophysics, Graduate School of Science, Kyoto University, Kyoto, Japan. [4]IRAP-CNRS-CNES-Toulouse University, Toulouse, France. [5]Institute of Space and Astronautical Science, Japan Aerospace Exploration Agency, Sagamihara, Japan. [6]Department of Physics, University of Pisa, Pisa, Italy. [7]Institut Supérieur de l'Aéronautique et de l'Espace (ISAE-SUPAERO), Université de Toulouse, Toulouse, France. [8]Department of Climate and Space Sciences and Engineering, University of Michigan, Ann Arbor, MI, USA. [9]Department of Earth and Space Science, Graduate School of Science, Osaka University, Osaka, Japan. [10]Max Planck Institute for Solar System Research (MPS), Göttingen, Germany. [11]IDA, Braunschweig, Germany. [12]LATMOS-CNRS-IPSL, Paris, France. [13]Institute of Science and Engineering, Kanazawa University, Kanazawa, Japan. ✉e-mail: lina.hadid@lpp.polytechnique.fr

group) were primarily observed in the region of the magnetospheric cusp on the dayside and near the equator in the nightside plasma sheet[10,12]. For these plasma populations, due to the limited mass resolution of the FIPS instrument, it was not possible to clearly differentiate ions within specific groups, e.g., to distinguish O^+ from water group ions or Na^+ from Mg^+. Moreover, FIPS had both restricted Field-of-View (due to the spacecraft thermal shield) and a limited energy range (spanning from approximately 50 eV e^{-1} up to about 13 keV e^{-1}); hence, some limitations on the characteristic energy of the ion plasma.

In 2021, 2022, and 2023, BepiColombo, a joint ESA/JAXA mission, conducted its first three flybys at Mercury as part of its cruise phase until December 2025 when the two spacecraft will go into orbit around Mercury[13,14]. In this context, we present measurements from the ion and electron sensors of the Mercury Plasma Particle Experiment (MPPE) consortium[15] onboard the Magnetospheric Orbiter (known as Mio). We focus on the third gravity assist maneuver (MFB3) that occurred on June 19, 2023. During this flyby, the spacecraft reached low altitudes, traveling down to ~235 km above the planet's surface. The ion plasma observations were recorded by the Mercury Ion Analyzer (MIA) and the Mass Spectrum Analyzer (MSA[16]), and the electron observations by one of the Mercury Electron Analyzers (MEA 2)[15]. We describe the characteristics of the plasma and highlight the mass-per-charge information collected by MSA along the BepiColombo trajectory near Mercury. We do not show any magnetic field data, as at the time of writing the manuscript the data are still under calibration. Note that MIA and MEA 2 are a top-hat energy analyzer that measures total ion and electron fluxes respectively, while MSA combines a spherical top-hat analyzer with a "reflectron" Time-Of-Flight (TOF) chamber to investigate the plasma composition with a high mass resolution[16]. MIA, MSA, and MEA2 will measure ions and electrons over about 4 π sr when Mio is spinning in the orbital phase. However, due to the "stacked configuration" of BepiColombo during cruise, the Magnetospheric Orbiter Sunshield and Interface Structure (MOSIF) significantly obstructs the Field-Of-View (FOV) of all the particle sensors. As a consequence, the FOVs of MIA, MSA, and MEA 2 are reduced to about 0.13, 0.1 π sr, respectively. As a matter of fact, only two entrance windows of the ion sensors that point along the +Z axis of BepiColombo are recording ion flux[15]. Moreover, it is worth noting that the ion thrusters are never operating during the flybys, hence not contaminating the ion observations.

The high mass resolution and broad energy range of MSA, MIA, and MEA 2 instruments onboard the magnetospheric orbiter revealed insights into the planet's plasma environment including additional evidence of the ring current observations made by previous spacecraft. This evidence comes from the first identification of trapped energetic hydrogen (H^+) with energies of around 20 keV e^{-1}. Cold ion plasma with energies below 50 eV has also been detected for the first time. In addition, the observations revealed the existence of a Low-Latitude Boundary Layer (LLBL), which is a region of turbulent plasma at the edge of the magnetosphere.

Results and discussion

BepiColombo's trajectory and boundaries identification

BepiColombo's third Mercury flyby occurred in a near-equatorial region, approaching the planet from dusk-nightside, passing through the post-midnight magnetosphere, and moving away towards dawn-dayside (see Fig. 1). The global structure and dynamics of Mercury's magnetosphere during MFB3 are clearly reflected in the time evolution of the Differential Directional Energy Flux (DDEF) of the ions and electrons measured by MSA, MIA and MEA, shown in Fig. 2. In the outermost region, the Bow Shock (BS) was crossed inbound at 18:44:22 Universal Time (UT) and outbound at 19:52:00 UT. In the dayside solar wind and the magnetosheath, before and after the BS crossings (Fig. 2, magenta vertical lines), ions with narrowband features of ~10 eV e^{-1} and ~20 eV e^{-1} are continuously observed. Examination of the mass-per-charge spectra (next section) reveals that these ions essentially have a mass-per-charge ratio m/q = 1 (H^+) and m/q = 16 (O^+), consistent with spacecraft outgassing of water group molecules as observed elsewhere during BepiColombo cruise phase[17]. The magnetopause, which separates the shocked solar wind in the magnetosheath from Mercury's magnetosphere, was crossed inbound at 19:14:00 UT and subsequently outbound at 19:45:00 UT (cyan vertical lines). Based on the location of the magnetopause[18], have reported the highly compressed nature of Mercury's magnetosphere during this third flyby, in comparison to the first two flybys.

Magnetospheric regions and ion composition

The low latitude boundary layer. We stress in Fig. 2a, b, the presence of an energy dispersion of the ions as the spacecraft enters the dusk magnetosphere (after the first cyan vertical line). This dispersion extends

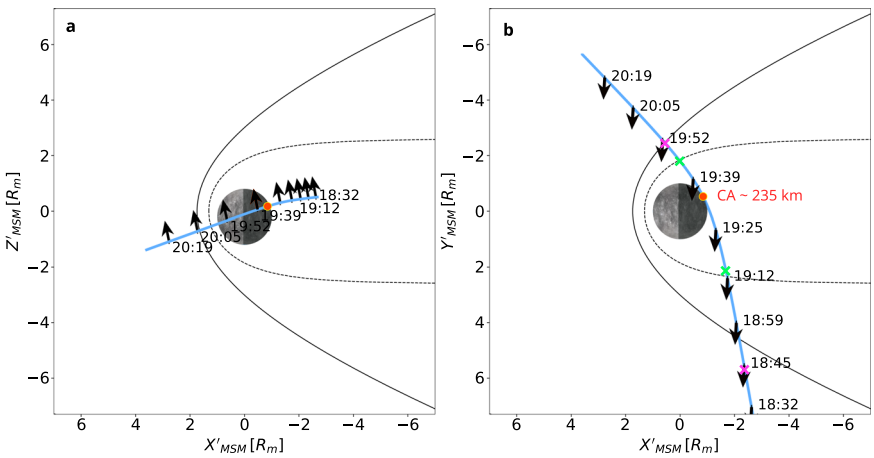

Fig. 1 | Projections of BepiColombo's third Mercury flyby trajectory in the aberrated Mercury–Sun magnetospheric (aMSM) coordinate system. a X'–Z' and (**b**) X'–Y' planes, all expressed in Mercury radii ($R_M \approx 2440$ km). Note the displacement in (**a**) of the magnetopause relative to the planetary center because of the northward offset of the magnetic dipole by ~0.2 R_M. In traditional MSM coordinates, the X-axis and Z-axis point to the sun and north pole, respectively, and the Y-axis completes a right-hand system. In the aberrated coordinates, Mercury's orbital velocity is considered. The X-axis is anti-parallel to the solar wind direction in the rest of the reference frame of Mercury. The aberration angle varies between −5.5° and −8.4° assuming a solar wind speed of 400 km/s. The black arrows indicate the viewing direction of MSA during this flyby. The magenta and cyan crosses represent the observed inbound (and outbound) bow shock and magnetopause crossings, respectively (see Fig. 2). The red dot highlights the closest approach of BepiColombo to Mercury. The black solid and dashed lines represent the modeled dayside bow shock and magnetopause that are obtained from the statistical distribution of observed crossing points[40], respectively.

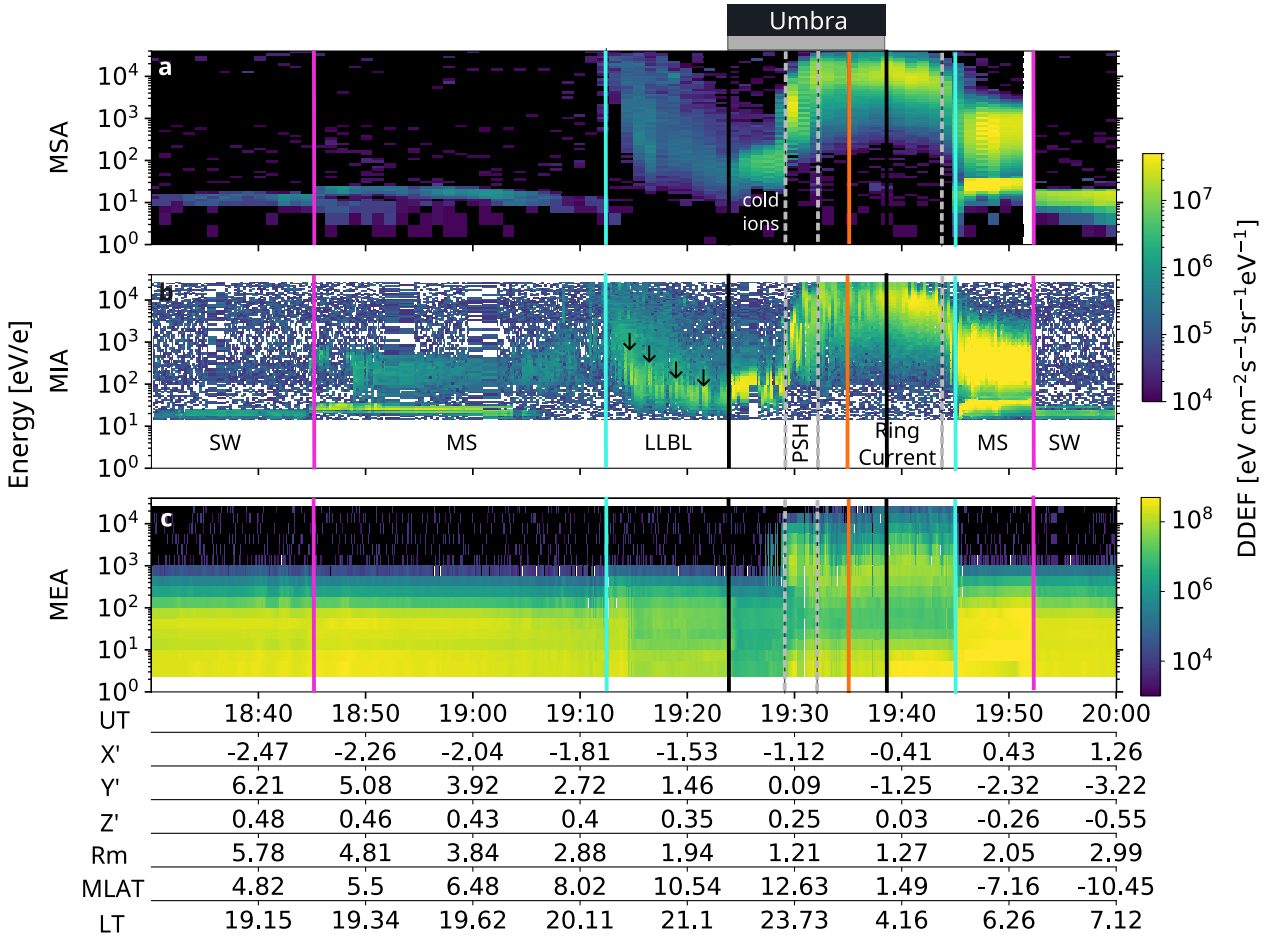

Fig. 2 | Energy-time spectrograms of the plasma measured during the third Mercury flyby. a shows the differential directional energy flux measured by the Mass Spectrum Analyzer (MSA). **b** shows the differential directional energy flux of the ions measured by the Mercury Ion Analyzer (MIA). shows the differential directional energy flux of the electrons observed by one of the Mercury Electron Analyzers (MEA 2) (**c**). X', Y', and Z' correspond to the location of the spacecraft in aberrated Mercury–Sun magnetospheric coordinate system. MLAT and LT represent the Magnetic Latitude and the Local Time respectively. The magenta, cyan, and red vertical lines represent the inbound (and outbound) bow shock, magnetopause, and closest approach respectively. The grey dashed lines, delimit the Low Latitude Boundary Layer (LLBL), Plasma Sheet Horns (PSH), and ring current regions. The black vertical lines delimit the period during which BepiColombo was in the planet Umbra. Impulsive enhancements of the ion flux inside the LLBL are noticeable (small black arrows), that imply the occurrence of injection processes.

from ~20 keV e^{-1} in the outermost part of the flank down to tens of eVs per e in the innermost part. We refer to this region as the LLBL, the region where magnetosheath and magnetospheric plasmas are mixed along the magnetospheric side of the low-latitude magnetopause. Such an energy dispersion is a characteristic feature of the plasma mantle at high latitudes[19], reflecting the different convection rates of high and low-energy ions. The fact that this energy dispersion is observed here in the near-equatorial region exemplifies the connection between the plasma mantle and the LLBL and highlights the role of magnetospheric convection in the transport of the ions into the deep magnetosphere of Mercury. Using backward test-particle simulations with an idealized magnetospheric model[20], H^+ ions detected in LLBL region seem to originate from the duskside magnetosphere (trajectories coded in green). In this analysis, test-particle simulations with static models of the magnetic and electric fields (refer to legend in Fig. 3) are utilized to illustrate prototypical ion behaviors and aid in the interpretation of their origin. It is important to highlight that these simulations are not the primary focus of the study. An in-depth analysis utilizing more comprehensive field models will be the subject of a separate future work. Note the temporary enhancements of the ion flux (indicated by small black arrows in Fig. 2c), suggesting of impulsive injection events in the duskside flank magnetosphere, akin to the Plasma Sheet Boundary Layer at Earth[21,22] or associated to other energization processes such as to Kelvin–Helmholtz instabilities or magnetic reconnection at the magnetopause boundaries. In addition to solar wind plasma, the LLBL may contain heavy ions originating from the planet. These ions can be transported from the dayside exosphere over the polar cap, as demonstrated by Delcourt et al.[20]. The interplay between several processes such as magnetic reconnection at high latitudes, Kelvin-Helmholtz instability, and the role of planetary ions in the formation of the LLBL in the Hermean environment[23,24] remains an open question and necessitates more detailed investigation, which is beyond the scope of this paper. Finally, in the inner LLBL region near 19:24:25 UT, the MSA and MIA instruments detected an intense cold ion signature between 30 eV e^{-1} and 100 eV e^{-1} while MEA 2 observed a strong depletion in the electron flux. This event occurred just as BepiColombo entered the shadow of Mercury, a region known as the umbra. With BepiColombo out of direct sunlight, the spacecraft likely acquires a negative charge. Low energy ions (typically, a few eV e^{-1}) of the ambient plasma are then accelerated toward the spacecraft and become "visible" to ion sensors, as described in ref. 25. We thus interpret the cold dense ions observed near 19:24:00 UT to be the product of spacecraft charging in the umbra, attracting very low energy ions originating from the planet surface possibly produced by sputtering from high energy magnetospheric ions[26] or simply related to the extension of the exosphere due to the solar radiation pressure (the Na tail). Because only TOF measurements integrated over 1024 s are available

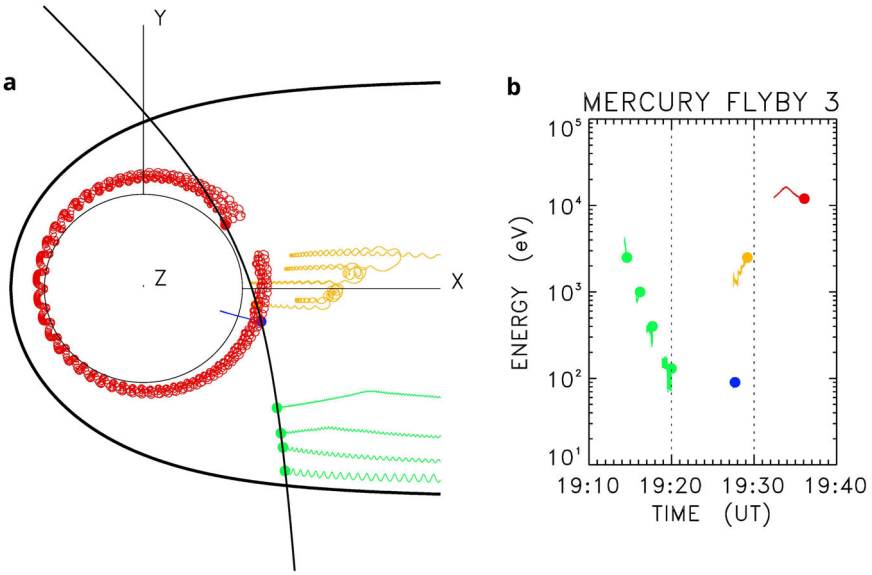

Fig. 3 | Model of the H^+ trajectories. a shows various particle trajectory projections in the equatorial plane traced backward in time. **b** shows the particle kinetic energy versus time. The ions are launched from different locations (closed circles) along BepiColombo's orbit and their trajectories are traced backward in time. The color code depicts the different magnetospheric regions, viz., the Low-Latitude Boundary Layer (LLBL) in green, the umbra in blue, the Plasma Sheet Horns (PSH) in yellow, and ring current in red. The test H^+ trajectories were computed using a modified Luhmann–Friesen model for the magnetic field combined with a two-cell convection pattern for the electric field[20]. The full equation of motion was integrated backward in time using a fourth-order Runge–Kutta technique.

during the cruise phase, the time resolution for ion species identification is fairly limited. However, by comparing the energy-time spectrograms of Fig. 2 with MSA TOF measurements, it is possible to acquire some insights into the ion species distribution inside the magnetosphere, as illustrated in Fig. 4c. Overall, the ion composition measurements suggest the dominance of protons that are likely of solar wind origin, nevertheless, a minor component of heavy ions are also observed. MSA measurements in the LLBL between 19:10:30 UT and 19:27:34 UT reveal the presence of heavy ions ($16 \le m/q \le 23$) with energies of about 10 keV e^{-1} or above, consistent with O^+ and Na^+. As shown in refs. 20,27, such ions of planetary origin may gain access to the dusk magnetospheric flank after being transported from the dayside exosphere over the polar cap. Figure 4c shows that cold heavy ions with $m/q = 16$ (O^+) and $m/q = 39$ (Ca^+ or K^+) and lighter cold ions (H^+ and He^{2+}) were also detected in the same region of space.

The plasmas sheet horns. Immediately after LLBL, 19:28:41 UT in Fig. 2, BepiColombo encounters a thermalized hot ion and for the first time electron populations of few keV e^{-1} in the near-tail plasma sheet. The presence of ~1 keV e^{-1} ions in the near-tail central plasma sheet extending to the higher latitudes is a characteristic feature of the "Plasma Sheet Horns" (PSH) reported by Glass et al. [28] using MESSENGER data in Mercury's northern magnetosphere. In this region where BepiColombo is traveling through, the ions are injected from the relatively distant tail and gradually accelerated up to several keV e^{-1} through convection toward the planet. The trajectory coded in yellow in Fig. 3 illustrates these behaviors.

The ring current. From about 19:32:00 UT until 19:44:04 UT (magnetic latitude ranging from −3° to 12°) in Fig. 2, the spacecraft travels through a region characterized by intense ion flux in the 5 keV e^{-1}–40 keV e^{-1} energy range and energetic electron flux up to 10 keV. The larger energy ranges of MIA and MSA, compared to MESSENGER FIPS, allow the full energy distribution of this population to be measured for the first time. The high-energy character of this ion population and its presence at both equatorial latitudes and low altitudes strongly suggest that BepiColombo is here traveling through Mercury's tenuous ring current. The existence of a ring current at Mercury has been debated in a variety of studies[29–31]; although simulation results and statistical analysis of MESSENGER data have suggested that protons could be quasi-trapped for one or more orbits from radial distances of ~1.3 R_M to ~1.5 R_M[32,33], the displacement of the magnetosphere down to the planet surface during events of prominent compression would preclude this trapping at least part of the time[34]. In view of this, the possibility of a partial ring current (i.e., extending within limited sectors of longitude) has been proposed. During MFB3, the detection of energetic protons suggests the existence of a ring current, as illustrated in Fig. 3, that displays the model trajectory (coded in red) of a 10 keV e^{-1} H^+ launched from BepiColombo position. With a subsolar stand-off distance located at 1.31 R_M in the magnetic field model, it is apparent from Fig. 3 that the test proton achieves a full drift around the planet in about 4 minutes. We note that the magnetic field model used in this code (see legend of Fig. 3) represents the average state of Mercury's magnetosphere with given magnetopause distance. Thus we do not take into account the interplanetary magnetic field configuration or the solar wind plasma parameters for this study. Moreover, it is worth noting that in contrast to the study of ref. 29 and since the drift paths of H^+ are not close enough to the magnetopause, their trajectory shown here is not bifurcated in the dayside sector due to the presence of a field minimum in the outer cusp region, as expected in Shabansky orbits[35]. In contrast, the test H^+ here bounces back and forth on either side of the equatorial plane throughout its motion around the planet. As compared to FIPS measurements onboard MESSENGER that were limited to about 13 keV e^{-1}, the MSA dataset shown in Fig. 2a provides more clear evidence of Mercury's ring current because of the wider energy range of the instrument (up to 40 keV e^{-1}). However, it is worth noting that the interpretation of a full or partial ring current cannot be definitively concluded with the limited FOV of the sensors and warrants further investigation. This will be possible during the orbital phase when MIA and MSA will measure the full 3D distribution of the ions. Figure 4 shows that, in the ring current region and around the closest approach during MFB3, the detected energetic ions consist of $1 \le m/q \le 4$ (H^+ and He^{2+}) and heavier population with $16 \le m/q \le 40$. Note that, these latter ones exhibit two distinctive bands, one ~2 keV e^{-1} predominantly O^+ (peaking at $m/q = 16$) and a second one at ~10 keV e^{-1} predominantly K^+ and Ca^+ (peaking at $m/q = 39$). These observations indicate that O^+ is the dominant heavy ion around the central plasma sheet with smaller contributions from Na^+ and K^+/Ca^+. This could be related to the limited field of FOV of MSA during cruise, which restrains the observation of Na^+ ions due to their anisotropic distribution. Moreover, as mentioned earlier, since MSA TOF spectra are integrated over 1024 s, it is unfortunately impossible to investigate the spatial m/q distribution further. Note that cold ions around ~15 eV e^{-1} with $16 \le m/q \le 23$ are also detected. Because of the low time resolutions of the TOF spectra of Straight-Through particles in Low mode (referred hereafter as TSTL), it is difficult

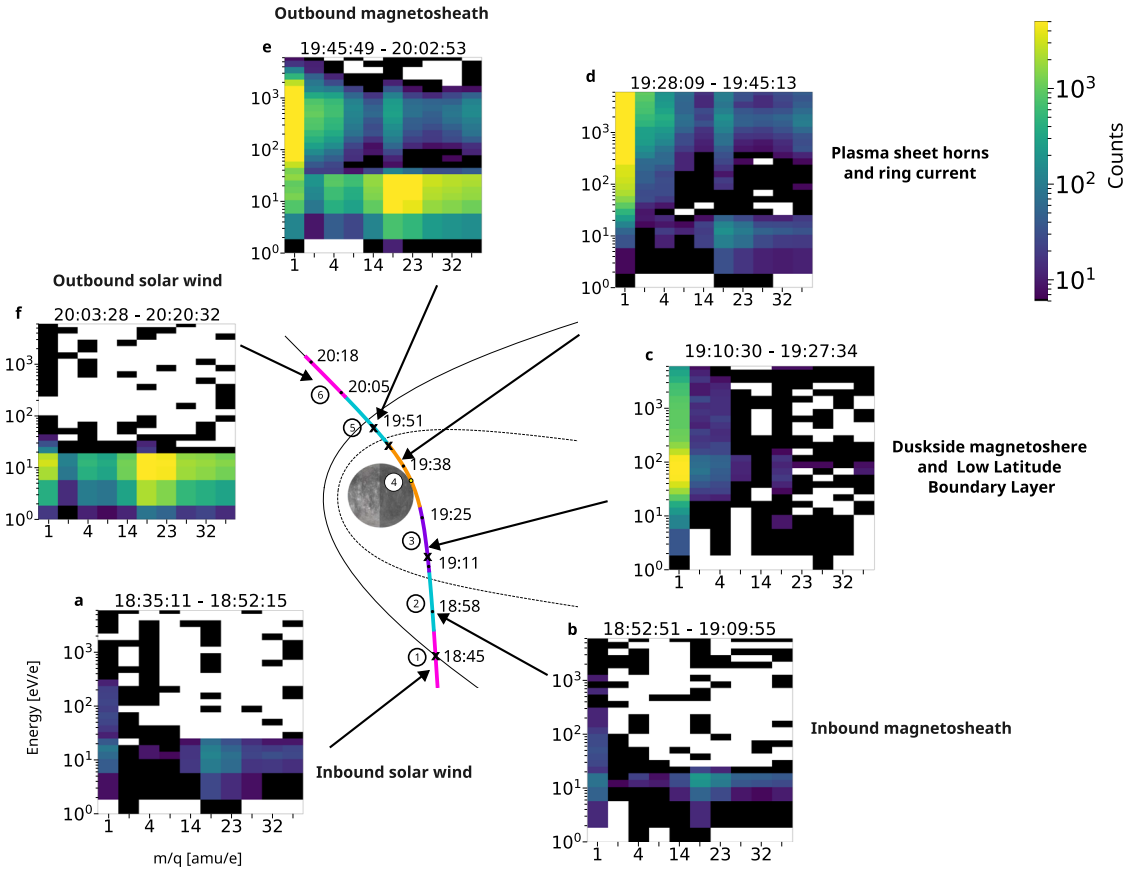

Fig. 4 | Spatial and mass-to-charge distribution of the ion species during Bepi-Colombo's third Mercury flyby. Ion energy versus mass-to-charge ratios (m/q) for different locations along BepiColombo orbit integrated over ~1024 s between (**a**) 18:35:11–18:52:15 in the inbound solar wind, (**b**) 18:52:51–19:09:55 in the inbound magnetosheath, (**c**) 19:10:30–19:27:34 in the duskside magnetosphere, (**d**) 19:28:09–19:45:13 passing through the plasma sheet horns and the ring current, (**e**) 19:45:49–20:02:53 in the outbound magnetosheath and (**f**) 20:03:28–202:20:32 in the outbound solar wind. The m/q ratios are derived from the Mass Spectrum Analyzer (MSA) Time-Of-Flight (TOF) measurements. The trajectory of BepiColombo is shown in the Mercury–Sun Magnetospheric (MSM) coordinate system projected in the X-Y plane (see Fig. 1 for definition of the MSM). The observation sequences of the TOF spectra of Straight-Through particles in Low mode (TSTL) are shown by the different colors along BepiColombo's trajectory numbered from 1 to 6. The black crosses denote the observed bow shock and magnetopause crossings.

to be conclusive on the origin of the these cold ions: they could be related to the outgassing observed from the outbound magnetosheath, or they could be of planetary origin. In fact, comparing these data with the energy-time spectrograms in Fig. 2 suggests that these ions could be observed ~332 km around 19:37 UT just after the closest approach.

The outbound magnetosheath and solar wind. Finally, after traveling by the post-midnight magnetosphere of Mercury, it is apparent from Fig. 2 that BepiColombo enters into the magnetosheath and then into the solar wind. In the dayside magnetosheath downstream of the BS, the solar wind plasma is highly compressed, heated, and deflected, and it can be seen in Fig. 4 that the plasma then essentially consists of H^+ and He^{2+} (a direct tracer of solar wind plasma). Also, the characteristic spacecraft outgassing signature with water group molecules is again detected outbound (Fig. 4e, f) with a clear change in the ion energy upon crossing the BS (Fig. 2).

Conclusions

Overall, the spatial distribution of the plasma around Mercury as measured by MSA, MIA, and MEA 2 Mio over a wider range of energies than MESSENGER, provides a rare dawn-dusk synoptic view of the large-scale structure of Mercury's magnetosphere that is not very different from Earth's. The ion observations highlight the presence of cold ions (≤50 eV e^{-1}) and energetic ions population (up to 38 keV e^{-1}) in the Hermean environment. Energetic electrons up to 10 keV e^{-1} were also observed in the deep magnetosphere. Such energetic ions play crucial role in the ion recycling in Mercury's magnetosphere, ie: ion sputtering producing secondary neutrals and ions from the planet's surface with different sputtering yields depending on the ion energetic[36]. Moreover, The presence of these low-energy ions of planetary origin would address the role of the heavy ions in the system (contribution to the plasma pressure, dynamics, etc.) which is one of the big questions that BepiColombo is going to address[37]. Moreover, original observations by MSA contribute to substantial additional evidence of a (partial or full) ring current encircling Mercury with characteristic energy of about 20 keV e^{-1}. MFB3 observations also reveal the existence of a Low-Latitude Boundary Layer with an impulsive injection process at work that leads to bursty enhancements of the ion flux that could be due to different energization processes, such as Kelvin-Helmholtz instabilities or ongoing magnetic reconnection at the magnetopause boundary. All of these regions of Mercury's magnetosphere and others will continue to be the subject of intensive study by the instruments of the MPPE suite through the remainder of BepiColombo's cruise and the orbital phase of the mission. The two-point measurements between Mercury Planetary Orbiter (MPO) and Mio will provide valuable insights into the dynamics and plasma transport in Mercury's magnetosphere.

Methods

MSA instruments

The Mass Spectrum Analyzer (MSA) onboard Mio, BepiColombo's magnetospheric orbiter, is an advanced ion spectrometer known for its high-mass resolution. Being part of the Mercury Plasma Particle Experiment (MPPE) consortium, which focuses on particle measurements[15], the MSA

aims to provide detailed three-dimensional mass-resolved ion phase space densities in Mercury's magnetosphere. This instrument combines a spherical top-hat analyzer for energy analysis with a Time-Of-Flight (TOF) chamber for mass analysis. When ions enter the TOF analyzer, they interact with carbon foils, undergoing charge exchange, which transforms them into neutrals, positive, or negative ions.

In contrast to other spacecraft spectrometers like MESSENGER's Fast Imaging Plasma Spectrometer (FIPS) with its equipotential TOF chamber[12,38], the MSA's TOF chamber is distinctively linearly polarized. This polarization allows for precise corrections of energy and angular scattering as positive ions enter the TOF chamber[16]. The use of the innovative "reflectron" concept[39] ensures isochronous TOF, thereby enhancing mass resolution ($m/\Delta m > 40$). Achieving such high levels of performance is uncommon among onboard mass spectrometers and is particularly advantageous at Mercury, where numerous ions of planetary origin traverse the magnetosphere due to phenomena such as solar wind sputtering, thermal desorption, and meteorite impacts.

Data availability

The spacecraft orbit data are available from SPICE data for BepiColombo. The MSA, MIA, and MEA 2 data are available in a Zenodo repository (https://doi.org/10.5281/zenodo.12804675) and in AMDA/CDPP websites. The MSA, MIA, and MEA teams (Yoshifumi Saito, principal investigator; saito@stp.isas.jaxa.jp) and the corresponding author can provide the data upon request.

Received: 10 July 2024; Accepted: 2 August 2024;
Published online: 03 October 2024

References

1. Slavin, J. Mercury's magnetosphere. *Adv. Space Res.* **33**, 1859–1874 (2004).
2. Slavin, J. A., Imber, S. M. & Raines, J. M. *A Dungey Cycle in the Life of Mercury's Magnetosphere*, chap. 34, 535–556 (American Geophysical Union (AGU), 2021).
3. Ness, N. F., Behannon, K. W., Lepping, R. P., Whang, Y. C. & Schatten, K. H. Magnetic field observations near Mercury: preliminary results from mariner 10. *Science* **185**, 151–160 (1974).
4. Broadfoot, A. L., Shemansky, D. E. & Kumar, S. Mariner 10: Mercury atmosphere. *Geophys. Res. Lett.* **3**, 577–580 (1976).
5. Potter, A. & Morgan, T. Discovery of sodium in the atmosphere of Mercury. *Science* **229**, 651–653 (1985).
6. Potter, A. & Morgan, T. Potassium in the atmosphere of Mercury. *Icarus* **67**, 336–340 (1986).
7. Bida, T. A., Killen, R. M. & Morgan, T. H. Discovery of calcium in Mercury's atmosphere. *Nature* **404**, 159–161 (2000).
8. Solomon, S. C. & Anderson, B. J. *The MESSENGER Mission: science and implementation overview*, 1–29. Cambridge Planetary Science (Cambridge University Press, 2018).
9. Zurbuchen, T. H. et al. Messenger observations of the composition of Mercury's ionized exosphere and plasma environment. *Science* **321**, 90–92 (2008).
10. Zurbuchen, T. H. et al. Messenger observations of the spatial distribution of planetary ions near Mercury. *Science* **333**, 1862–1865 (2011).
11. Raines, J. M. et al. Messenger observations of the plasma environment near Mercury. *Planet. Space Sci.* **59**, 2004–2015 (2011).
12. Raines, J. M. et al. Distribution and compositional variations of plasma ions in Mercury's space environment: The first three Mercury years of messenger observations. *J. Geophys. Res.* **118**, 1604–1619 (2013).
13. Milillo, A. et al. Investigating Mercury's environment with the two-spacecraft BepiColombo mission. *Space Sci. Rev.* **216**, 93 (2020).
14. Benkhoff, J. et al. BepiColombo—mission overview and science goals. *Space Sci. Rev.* **217**, 90 (2021).
15. Saito, Y. et al. Pre-flight calibration and near-earth commissioning results of the Mercury plasma particle experiment (MPPE) onboard MMO (Mio). *Space Sci. Rev.* **217**, 70 (2021).
16. Delcourt, D. et al. The mass spectrum analyzer (MSA) on board the Bepicolombo MMO. *J. Geophys. Res.* **121**, 6749–6761 (2016).
17. Franz, M. et al. Spacecraft outgassing observed by the BepiColombo ion spectrometers. *J. Geophys. Res.* **129**, e2023JA032044 (2024).
18. Rojo, M. et al. Structure and dynamics of the Hermean magnetosphere revealed by electron observations from the Mercury electron analyzer after the first three Mercury flybys of BepiColombo. *AA* **687**, A243 (2024).
19. DiBraccio, G. A. et al. First observations of Mercury's plasma mantle by messenger. *Geophys. Res. Lett.* **42**, 9666–9675 (2015).
20. Delcourt, D. C. et al. A quantitative model of the planetary Na^+ contribution to Mercury's magnetosphere. *Ann. Geophys.* **21**, 1723–1736 (2003).
21. Keiling, A. et al. New properties of energy-dispersed ions in the plasma sheet boundary layer observed by cluster. *J. Geophys. Res.* **109**, https://doi.org/10.1029/2003JA010277 (2004).
22. Ashour-Abdalla, M. et al. A stochastic sea: The source of plasma sheet boundary layer ion structures observed by cluster. *J. Geophys. Res.* **110**, https://doi.org/10.1029/2005JA011183 (2005).
23. Slavin, J. A. et al. Messenger and Mariner 10 flyby observations of magnetotail structure and dynamics at Mercury. *J. Geophys. Res.* **117**, https://doi.org/10.1029/2011JA016900 (2012).
24. Liljeblad, E. et al. Messenger observations of the dayside low-latitude boundary layer in Mercury's magnetosphere. *J. Geophys. Res.* **120**, 8387–8400 (2015).
25. Seki, K. et al. Cold ions in the hot plasma sheet of earth's magnetotail. *Nature* **422**, 589–592 (2003).
26. Leblanc, F., Delcourt, D. & Johnson, R. E. Mercury's sodium exosphere: magnetospheric ion recycling. *J. Geophys. Res.* **108**, https://doi.org/10.1029/2003JE002151 (2003).
27. Delcourt, D. C. On the supply of heavy planetary material to the magnetotail of Mercury. *Ann. Geophys.* **31**, 1673–1679 (2013).
28. Glass, A. N. et al. Observations of Mercury's plasma sheet horn: characterization and contribution to proton precipitation. *J. Geophys. Res.* **127**, e2022JA030969 (2022).
29. Zhao, J.-T. et al. Observational evidence of ring current in the magnetosphere of Mercury. *Nat. Commun.* **13**, 924 (2022).
30. Shi, Z. et al. An eastward current encircling Mercury. *Geophys. Res. Lett.* **49**, e2022GL098415 (2022).
31. Fu, S. & Zong, Q. Mercury's ring current and Mercury's magnetic storms. *Sci. China Technol. Sci.* **65**, 1210–1212 (2022).
32. Trávníček, P. M. et al. Mercury's magnetosphere-solar wind interaction for northward and southward interplanetary magnetic field: Hybrid simulation results. *Icarus* **209**, 11–22 (2010).
33. Schriver, D. et al. Quasi-trapped ion and electron populations at Mercury. *Geophys. Res. Lett.* **38**, https://doi.org/10.1029/2011GL049629 (2011).
34. Slavin, J. A. et al. Messenger observations of Mercury's dayside magnetosphere under extreme solar wind conditions. *J. Geophys. Res.* **119**, 8087–8116 (2014).
35. Shabansky, V. P. Some processes in the magnetosphere. *Space Sci. Rev.* **12**, 299–418 (1971).
36. Poppe, A. R. & Curry, S. M. Martian planetary heavy ion sputtering of Phobos. *Geophys. Res. Lett.* **41**, 6335–6341 (2014).
37. Gershman, D. J. et al. Ion kinetic properties in Mercury's pre-midnight plasma sheet. *Geophys. Res. Lett.* **41**, 5740–5747 (2014).
38. Solomon, S. C., McNutt, R. L., Gold, R. E. & Domingue, D. L. Messenger mission overview. *Space Sci. Rev.* **131**, 3–39 (2007).
39. Managadze, G. G. Time-of-flight mass-spectrometer (1991).
40. Winslow, R. M. et al. Mercury's magnetopause and bow shock from messenger magnetometer observations. *J. Geophys. Res.* **118**, 2213–2227 (2013).

Acknowledgements
The authors express their sincere thanks to all members of the Mio and BepiColombo mission for their careful contributions to the projects' operations and for their efforts in making the mission successful. This paper is based on observations obtained with BepiColombo, a joint European Space Agency (ESA)-Japan Aerospace Exploration Agency (JAXA) science mission with instruments and contributions directly funded by the ESA Member States and JAXA. The French participation in the BepiColombo mission is funded by the Centre National d'Etudes Spatiales (CNES). Work at MPS was supported by the German Space Agency DLR under contracts 50 QW 0503, 50 QW 1303, 50 QW 1702, 50 QW 2101, and by the Max Planck Society.

Author contributions
L.Z.H. and D.D. developed the scientific content of the study, analyzed the data, and wrote the initial draft of the manuscript. Y.H., M.R., S.A. Y.S., N.A., A.N.G., J.M.R., M.F., F.L., R.M, D.F., N.K., H.K., Frédéric L., H.F., J.-J.B., J.-A.S, and S.M. have read and provided feedback on the manuscript. B.K., C.V., and B.F. have updated and validated the software of MSA. S.Y. has conducted laboratory tests to validate the software of MSA. Y.S. is the Principal Investigator of the Mercury Plasma Particle Experiment (MPPE) consortium. N.A. is Co-Principal Investigator of MPPE and PI of MEA. L.Z.H. is lead Co-Investigator of MPPE and PI of MSA. G.M. is JAXA's Project Scientist of BepiColombo Mio.

Competing interests
The authors declare no competing interests.

Additional information
Correspondence and requests for materials should be addressed to Lina Z. Hadid.

Peer review information This manuscript has been previously reviewed at another Nature Portfolio journal. The manuscript was considered suitable for publication without further review at *Communications Physics*.